THE EFFECT OF GEOMETRY ON THE PERFORMANCE OF SYNTHETIC JET ACTUATORS

M. Jabbal, H. Tang and S. Zhong
School of Mechanical, Aerospace and Civil Engineering
University of Manchester, UK

Keywords: *Synthetic Jet, Flow Control, Vortex Circulation*

Abstract

PIV measurements have been undertaken to investigate the effects of varying orifice depth (h) and cavity height (H) on the vortex circulation of round synthetic jets in quiescent conditions. It is found that at the same stroke length, the normalized vortex circulation increases rapidly with a decreasing h when h/D_o is less than 1. At h/D_o equivalent to 0.5, a peak in the normalized circulation is observed suggesting that this is the optimum configuration in the current actuator design for maximum circulation production. An increase in cavity height is observed to increase the normalized vortex circulation. It is believed that Helmholtz resonance plays a role in this trend. The findings from this study provide useful information for optimizing the design of synthetic jet actuators.

1 Introduction

The synthetic jet actuator (SJA) provides a novel means of applying flow control and its potential application for the delay of boundary layer separation on aircraft has been the focus of intense research in recent years. One of the reasons for this is due to its unique ability to impart additional momentum and vorticity on a fluid region from which it was originally synthesized without a net mass flux addition, thereby requiring no bleed air supply and piping.

A typical SJA, as shown in Fig.1 consists of a cylindrical cavity (with a diameter D_c and height H) bounded by rigid side walls with an oscillating diaphragm clamped at one end and an orifice plate (with a depth h and orifice diameter D_o) at the other. As a result of a periodic motion in suction and expulsion, a jet is synthesized from a train of vortex rings that propagate away from the orifice plate. The roll up and advection of vortex rings is a distinct characteristic of round synthetic jets, with the ensuing development of vortex circulation being a key performance parameter for potential flow control applications.

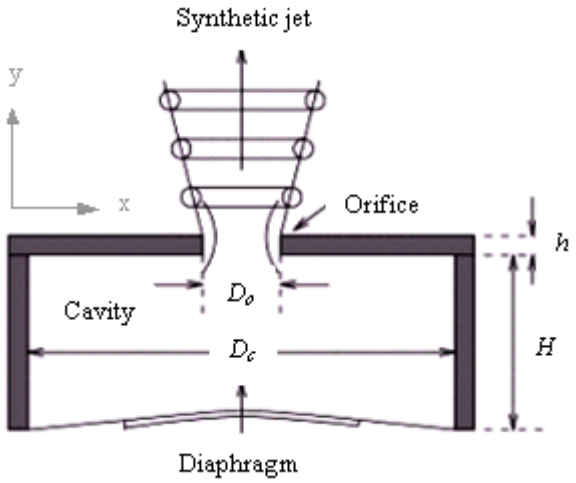

Fig 1. Schematic of a synthetic jet actuator

In order to optimize the design and effectiveness of a SJA for maximum circulation production, the effects of actuator geometry and operating conditions on the synthetic jet performance parameters should be fully understood. Tang and Zhong [1] developed a performance prediction model for round synthetic jets in quiescent conditions at the University of Manchester to obtain analytical relations of the SJA performance parameters with the operating conditions at a given actuator

geometry. Validation of the model was initially undertaken by the authors using CFD [1] and subsequently by Jabbal *et al* using PIV analysis [2]. Further numerical simulations were undertaken by Tang and Zhong [3] to investigate the effects of changing actuator geometry (namely H, h and D_c) on the strength of vortex roll up and hence the magnitude of vortex circulation of round synthetic jets. It was found that at a given diaphragm displacement, the normalized vortex circulation increased with decreasing H and h, whilst the effect of D_c was seen to be negligible. Their findings were in agreement with the DNS results of Rizetta *et al* [4], who computed synthetic jets from 2D slots and found the strength of the vortex pair increases with reducing cavity height at fixed diaphragm displacements. Lee and Goldstein [5] also obtained similar results and believed that the vorticity inside a shallow cavity may be pushed out of the orifice enhancing the vortex roll up. However, the aforementioned findings are contrary to the smoke visualizations carried out by Crook and Wood [6] who observed that an increase in the cavity height and orifice depth results in an increase in the circulation of a vortex ring.

Hence the work presented here aims at quantifying and understanding the effect of actuator geometric parameters (h and H) on the vortex circulation of round synthetic jets in quiescent flow, facilitated by PIV measurements. To simplify the task, the orifice diameter D_o and cavity diameter D_c are fixed for all test cases. It is anticipated that the experimental data obtained in this study will provide clarification on the impact of changing actuator geometry on the vortex circulation as well as providing useful information for optimizing the design of SJAs for enhanced flow control effectiveness.

2 Parametric Study of a Round Synthetic Jet

2.1 Dimensional Analysis

For a synthetic jet in quiescent conditions, the total circulation produced at the orifice will govern the dynamics and structure of the vortex rings. The flow from the actuator and hence the vortex circulation can be expressed as a function of 8 parameters in total – 2 operating parameters: oscillatory frequency f and diaphragm displacement Δ; 4 geometric parameters: orifice diameter D_o, cavity diameter D_c, orifice depth h and cavity height H and 2 fluid parameters: ambient density ρ and kinematic viscosity υ. Therefore:

$$\Gamma = fn\,(f, \Delta, D_o, D_c, h, H, \rho, \upsilon) \qquad (1)$$

or

$$g(\Gamma, f, \Delta, D_o, D_c, h, H, \rho, \upsilon) = 0 \qquad (2)$$

According to the Buckingham Pi theorem, if ρ, D_o and f are chosen as the basic 'repeating' variables (representing mass [M], length [L] and time [T] respectively) then it can be shown that

$$\frac{\Gamma}{fD_o^2} = fn\left(\frac{fD_o^2}{\upsilon}, \frac{D_c}{D_o}, \frac{h}{D_o}, \frac{H}{D_o}, \frac{\Delta}{D_o}\right) \qquad (3)$$

2.2 Jet Flow Characteristics

Smith and Glezer [7] have previously shown that for synthetic jets created by a sinusoidal motion in a quiescent flow, there are two independent dimensionless parameters that describe the nature of the jet, namely the dimensionless stroke length L and the jet Reynolds number Re. According to the slug model [8], the stroke length L_o represents the length of the column or 'slug' of fluid pushed out of the orifice during the blowing stroke. As defined by Equation (4) the stroke length is divided by the orifice diameter D_o to give L

$$L = \frac{L_o}{D_o} = \frac{\bar{U}_o}{fD_o} \qquad (4)$$

where $\bar{U}_o$ is the time-averaged blowing velocity over the entire cycle. The Reynolds number based on the time-averaged blowing velocity and orifice diameter is defined as

$$\mathrm{Re} = \frac{\bar{U}_o D_o}{\upsilon} \qquad (5)$$

In order to evaluate L and Re, $\bar{U}_o$ should be found. In the present investigation, the diaphragm is clamped round its edge and the displacement at its centre is fixed at a known value. Tang and Zhong [1] derived the instantaneous shape of the diaphragm that undergoes a sinusoidal motion according to the theory of thin shell as

$$\delta(r,t) = \frac{\Delta}{2}\left[1 - \frac{r^2}{r_c^2} + \frac{2r^2}{r_c^2}\ln\left(\frac{r}{r_c}\right)\right]\mathrm{Sin}(2\pi ft) \qquad (6)$$

where δ is the diaphragm deformation relative to its neutral position and r is the radial distance from the diaphragm centre. The derivative of Equation (6) with respect to time gives the oscillation velocity of the diaphragm.

For an incompressible flow and based on mass conservation in the cavity, the instantaneous space-averaged velocity at the orifice exit can be obtained

$$\tilde{u}_o(t) = \frac{\dot{Q}_o(t)}{\rho A} = \frac{\pi}{4} f\Delta\left(\frac{D_c}{D_o}\right)^2 \mathrm{Sin}(2\pi ft) \qquad (7)$$

where $\dot{Q}_o(t)$ is the instantaneous mass flow rate displaced by the diaphragm and expelled through the orifice with a geometric area A. Hence the time-averaged blowing velocity over the entire cycle can be found as

$$\bar{U}_o = \frac{1}{T}\int_0^{T/2} \tilde{u}_o(t)dt = \frac{1}{4} f\Delta\left(\frac{D_c}{D_o}\right)^2 \qquad (8)$$

Subsequently, using Equation (8), L and Re can be redefined as

$$L = \frac{L_o}{D_o} = \frac{1}{4}\left(\frac{\Delta}{D_o}\right)\left(\frac{D_c}{D_o}\right)^2 \qquad (9)$$

$$\mathrm{Re} = \frac{1}{4}\left(\frac{\Delta f D_o}{\upsilon}\right)\left(\frac{D_c}{D_o}\right)^2 \qquad (10)$$

In the present study where the effect of varying h, H and Δ on the vortex circulation is investigated whilst keeping D_o, D_c and f fixed, then it is seen that both L and Re are directly proportional to Δ.

According to Glezer [8], using a boundary layer approximation, the vorticity flux across the orifice exit plane (or the total circulation Γ_o) can be evaluated

$$\Gamma_o = \int_0^{T/2} \frac{u_o^2(0,t)}{2} dt \qquad (11)$$

where $u_o(0,t)$ is the axial velocity at the centre of the orifice exit. Equation (11) indicates that the total circulation is related to the time integral of the square of the instantaneous velocity at the orifice centre. Replacing $u_o(0,t)$ by the space-averaged velocity over the orifice $\tilde{u}_o(t)$, an approximate total circulation can be obtained

$$\Gamma_o \approx \int_0^{T/2} \frac{\tilde{u}_o^2(t)}{2} dt = \frac{\pi^2}{128}\Delta^2 f\left(\frac{D_c}{D_o}\right)^4 \qquad (12)$$

In order to allow for a comparison of the results obtained at different displacements, the calculated vortex can be normalized by the theoretically predicted total circulation Γ_o, as defined in Equation (12). Therefore in summary, Equation (3) may be simplified to

$$\frac{\Gamma}{\Gamma_o} = fn\left(\frac{h}{D_o}, \frac{H}{D_o}, \frac{\Delta}{D_o}\right) \qquad (13)$$

3 Experimental Method

In order to facilitate PIV measurements for an evaluation of the effect of actuator geometry on the performance of synthetic jets, a purpose-built rig was constructed. The SJA is of a modular design, thereby allowing orifice plates and cavities of different geometries to be interchanged with ease. An exploded view of the SJA is shown in Fig 2. The actuator consists of an orifice plate, which is clamped around its edge in succession to a cylindrical cavity, a thin

brass shim, 0.1mm thick, which acts as the diaphragm and finally a base plate. The underside of the diaphragm is attached via a steel rod to a permanent magnetic shaker, which oscillates the diaphragm with a sinusoidal waveform of an oscillatory frequency f, and peak-to-peak displacement Δ, supplied by a signal generator. An eddy current displacement sensor was used in the present investigation to accurately define the diaphragm displacement.

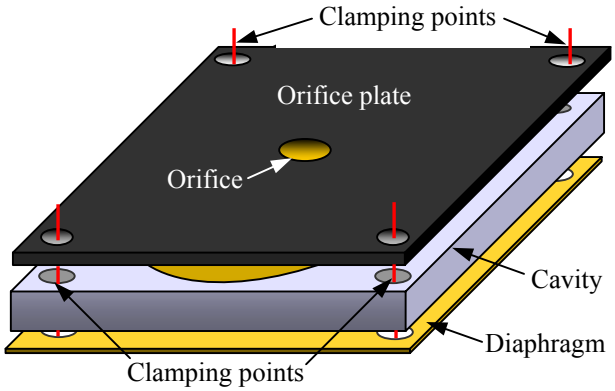

Fig 2. Modular construction of SJA

In total, 26 cases were investigated as listed in Table 1. Orifice plates with depths, h, of 1.25, 2.5, 5 and 10mm (corresponding to $0.25D_o$, $0.5D_o$, $1D_o$ and $2D_o$ respectively) and cylindrical cavities with depths, H, of 5, 10 and 20mm (corresponding to $1D_o$, $2D_o$ and $4D_o$ respectively) were tested. To simplify comparisons, the orifice diameter D_o, was fixed at a relatively large value of 5mm for all orifice plates. The cavity diameter D_c, was also fixed at 45mm for all cavities. In this study, the baseline case has an actuator geometry of h=$1D_o$ and H=$2D_o$, which is the same actuator as the one used by the authors previously in quiescent conditions [2].

For each case, the oscillatory frequency was fixed at f=100Hz whilst the diaphragm displacement was set at Δ=0.5, 0.8 and 1.1mm corresponding to dimensionless stroke lengths L, of 2.0, 3.2 and 4.4 respectively. Since Δ exhibits a linear relationship with the dimensionless stroke length and Reynolds number Re, at a fixed frequency and orifice diameter, the variations in diaphragm displacement allow the effect of changing geometry on the performance of SJAs to be examined for a range of L (or Re).

h/D_o	H/D_o	Δ (mm)	L	Re
0.25, 0.5, 1 & 2	1, 2 & 4	0.5	2.025	349
		0.8	3.240	559
		1.1	4.455	768

Table 1. Summary of test cases

To facilitate PIV measurements of synthetic jets, the SJA shown in Fig 2 was enclosed within a box comprising a glass window for optical access. A smoke generator was used to generate and seed the enclosed ambient air with finely dispersed oil droplets (~ 5 microns). The SJA flow field was illuminated by a TSI dual head Nd:YAG laser, operated with pulse energy of 200mJ and a pulse repetition rate of 5Hz. A light sheet less than 1mm in width was generated and directed across the orifice in the x-y plane (according to the coordinates in Fig 1) to produce a two-dimensional slice of the synthetic jet. A TSI PowerView CCD camera with a resolution of 2048×2048 pixels was used to capture vector fields in a field of view of 35mm×35mm. The vector fields were resolved using a two-frame cross-correlation algorithm in TSI Insight 3G. A 32×32-pixel interrogation area with an overlap ratio of 50% was chosen giving a spatial resolution of 0.3mm. The PIV system was synchronized with the periodic motion of the diaphragm so that measurements could be taken at 24 phases equally spaced across the diaphragm cycle, giving a temporal resolution of 15°. For a given phase point, phase-average flow fields were obtained by averaging 100 instantaneous image pairs.

4 Results & Discussion

4.1 Effect of Orifice Depth

From the phase-averaged velocity field obtained by PIV, the vortex circulation Γ can be calculated by integrating the vorticity over a region containing the primary vortex. This is

normalized by the theoretically predicted total circulation Γ_o, as defined in Equation (12) to compare the results at different diaphragm displacements. In accordance with Equation (13), the dependency of the normalized vortex circulation Γ/Γ_o, on h/D_o is plotted in Fig. 3.

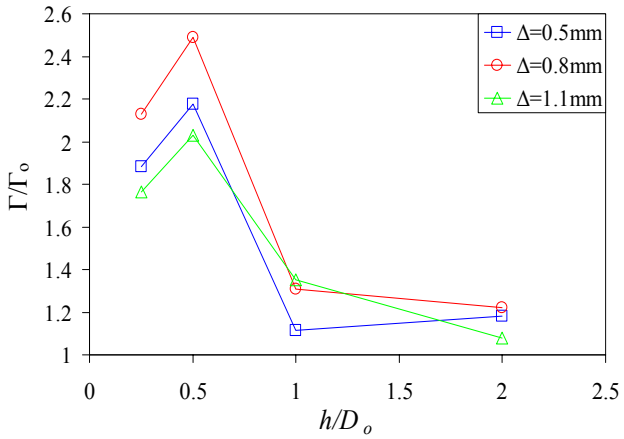

Fig 3. Correlation between normalized vortex circulation and h/D_o for H/D_o=2

As shown in Fig. 3 for the three displacements tested, Γ/Γ_o appears to be constant when h/D_o is greater than 1 but increases rapidly when h/D_o decreases from 1 and reaches a maximum at h/D_o=0.5. An examination of the phase-averaged vorticity contours at the instant when the vortex ring reaches its maximum strength, as shown in Fig. 4, confirms that the size of the vortex structure and thus the vortex roll up is at its greatest for h/D_o=0.5 compared to that at h/D_o=0.25 and 1. Similar results are also observed for H/D_o=1 in Fig. 5 with the highest vortex circulation occurring at h/D_o=0.5.

In order to provide an explanation for the observed effect of changing orifice depth on vortex circulation, the flow pattern in the orifice is examined using CFD simulations. The flow behaviour through the orifice is very complex. It firstly experiences a sudden contraction, as the fluid in the cavity is squeezed into the orifice and then undergoes expansion as the fluid is expelled from the orifice duct to the ambient surroundings. It is believed that flow separation takes place at the orifice inlet and outlet where a sudden change in the cross-sectional area occurs. The aforementioned flow features are captured well in the simulations shown in Fig 6.

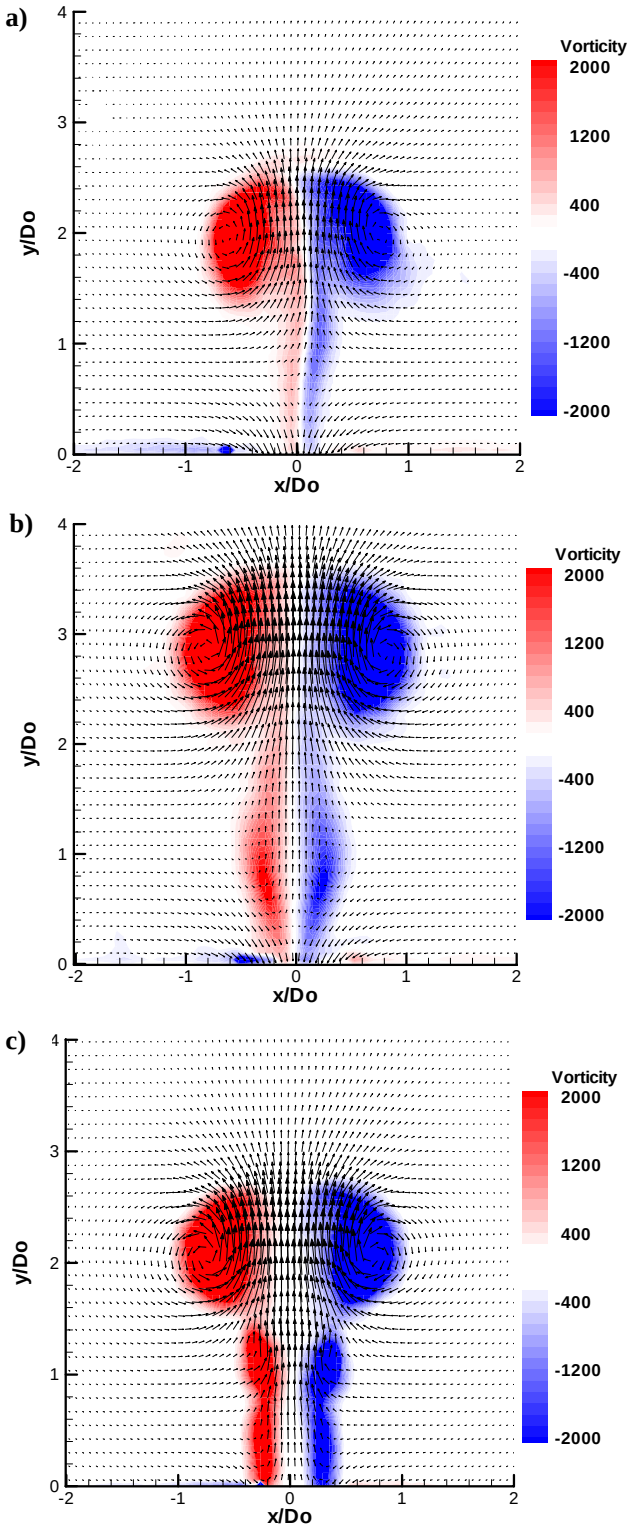

Fig 4. Contours of maximum vorticity for a) h/D_o=1, b) h/D_o=0.5 and c) h/D_o=0.25 at H/D_o=2 and Δ=0.8mm

Fig. 6 shows the velocity vector field in the orifice duct at the instant when the centerline velocity at the orifice exit reaches its maximum for different orifice depths. It is seen

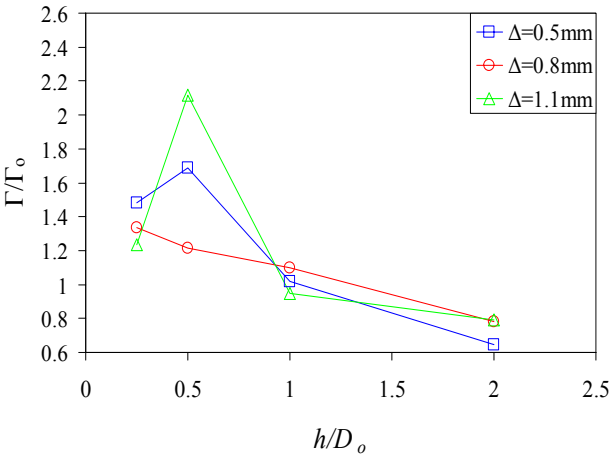

Fig 5. Correlation between normalized vortex circulation and h/D_o for H/D_o=1

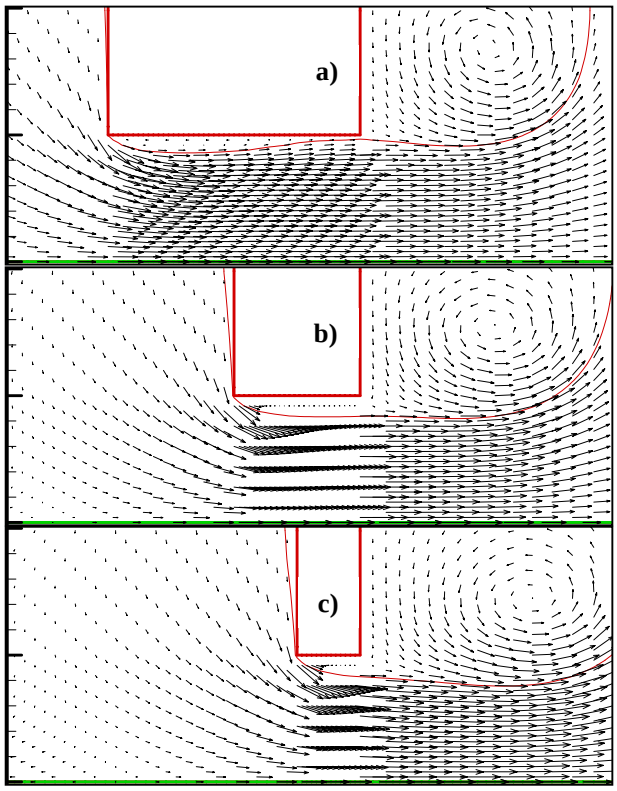

Fig 6. Flow pattern in the orifice corresponding to the maximum blowing phase for a) h/D_o=1, b) h/D_o=0.5 and c) h/D_o=0.25 at H/D_o=2 and Δ=0.8mm [3]

that flow separation occurs at the inlet of the orifice duct and the extent of this separation zone varies with the length of the orifice duct hence affecting the characteristics of vortex roll up and circulation. A virtual pipe bounded by the separating streamlines has a diameter smaller than the orifice diameter. The location of this minimum diameter is called the Vena Contracta. At h/D_o=1 (Fig. 6a), the Vena Contracta is located inside the orifice duct hence producing little influence on the exit velocity profile. As h decreases further, flow reattachment ceases to occur and the Vena Contracta moves out of the orifice exit (Figs. 6b & c). As such, the virtual exit diameter becomes smaller than that of the orifice and a higher velocity gradient in the separating shear layer results, producing higher vortex circulation. Nevertheless, the virtual exit diameter will not decrease continually as the orifice depth decreases since at the extreme case of h/D_o=0 it will become equal to D_o. Therefore, the virtual exit diameter should acquire its smallest value at a certain value of h/D_o thus giving rise to an optimal orifice depth that produces the maximum vortex circulation. This feature is strongly supported in the PIV analysis (Figs. 3 and 5), which shows that the optimal orifice depth for this actuator design is h/D_o=0.5.

In addition to these findings, the instantaneous velocity profiles corresponding to the maximum jet blowing phase for the cases shown in Figs. 3 and 6 were obtained from the PIV analysis and plotted in Fig. 7. The profiles confirm that the maximum velocity output that gives rise to the maximum vortex circulation is attained at h/D_o=0.5. For both h/D_o=0.25 and h/D_o=0.5, the velocity gradients near to the orifice walls are high and comparable to each other, hence the similar levels of circulation produced by both configurations in comparison to those with larger orifice depths (Figs. 3 and 4). Interestingly, for both h/D_o=0.25 and h/D_o=0.5 regions of reversed flow can be observed in the trends at $-0.5<x/D_o<-0.4$ and $0.4<x/D_o<0.5$. Subsequently, the velocity profiles initiate inboard of the orifice walls, depicting a narrowing of the jet in both cases. Thus, the velocity profiles are seen to capture the feature of a virtual pipe bounded by regions of separated flow that was seen in the CFD simulations (Figs. 6b & c). For the larger orifice depths (h/D_o=1 and h/D_o=2), the exit profiles initiate from the walls of the orifice, indicating that the flow is attached to orifice lining, as similarly shown by Fig. 6a.

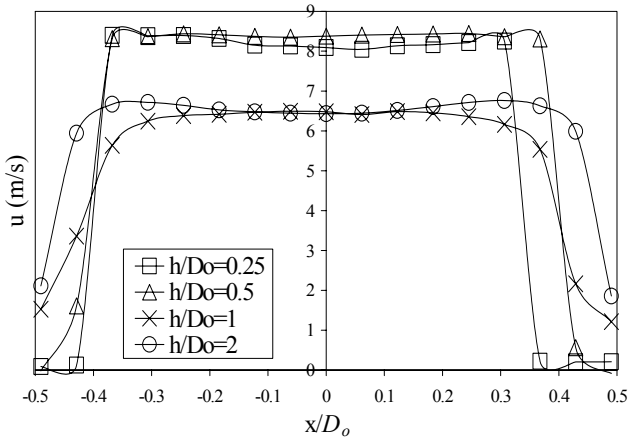

Fig 7. Instantaneous maximum blowing velocity profiles for different h/D_o at H/D_o=2 and Δ=0.8mm

4.2 Effect of Cavity Height

Fig. 8 shows the variation of the normalized vortex circulation with cavity height for two different diaphragm displacements. The experimental data shows that the vortex circulation increases as H/D_o increases from 1 to 4. The result is also confirmed by the instantaneous velocity profiles corresponding to the maximum jet blowing phase plotted in Fig. 9, which shows that the maximum velocity output that gives rise to the maximum vortex circulation is attained at H/D_o=4.

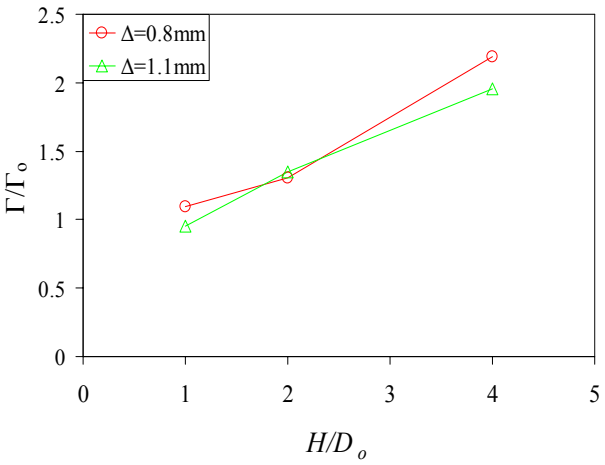

Fig 8. Correlation between normalized vortex circulation and H/D_o for h/D_o=1 obtained from PIV

Despite agreement with the qualitative observations made by Crook and Wood [6], the results seem to contradict previous numerical studies [4], [5], including the CFD results obtained by Tang and Zhong [3] using a dynamic incompressible model. The model predicted a gradual increase in vortex circulation with a decreasing H/D_o when H/D_o is less than 2 and a near constant vortex circulation when H/D_o is greater than 2. As such, this contradiction between the experimental findings and simulation prompts a consideration of the potential effects of Helmholtz resonance in the actuator design of the current investigation.

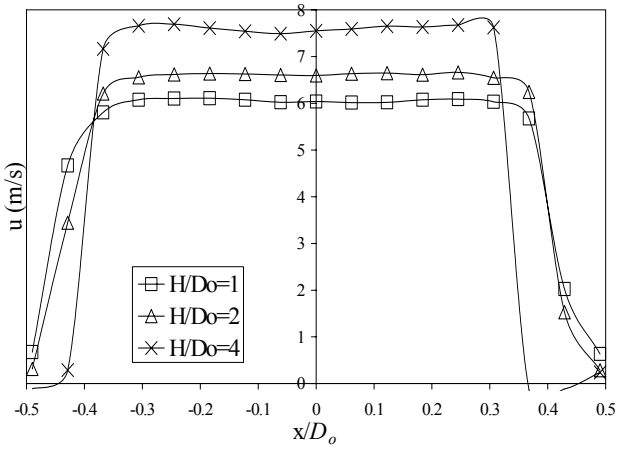

Fig 9. Instantaneous maximum blowing velocity profiles for different H/D_o at h/D_o=1 and Δ=0.8mm

Consider a container of air with an orifice. If disturbed, the volume of air in the orifice tends to vibrate at a certain frequency due to the 'springiness' of the air inside the container. This resonant frequency is referred to as the Helmholtz frequency and is dependent upon the geometry of the container and orifice as well as the fluid properties of the air. Consisting of a cavity with an orifice and an oscillating diaphragm that provides a continuous source of excitation, a SJA can be regarded as a Helmholtz resonator. The Helmholtz frequency f_H, of a SJA [9] is given by

$$f_H = \frac{a}{2\pi}\frac{D_o}{D_c\sqrt{Hh'}} \qquad (14)$$

where a is the speed of sound and h' is the effective orifice depth defined as $h'=h+0.8D_o$. At the Helmholtz frequency, a small pressure variation in the cavity is amplified to produce a large mass flow through the orifice. Hence for a

given SJA, a high jet peak velocity will be obtained if the diaphragm vibrates at the Helmholtz frequency.

For the baseline actuator case (i.e. h=1D_o and H=2D_o) the Helmholtz frequency according to Equation (14) is approximately 630Hz and decreases to 450Hz when the cavity height is doubled, thereby moving towards a frequency of 100Hz, as tested in the present study. Therefore, a likely explanation for the rise in vortex circulation with increasing cavity height observed in the experiment is that the actuator is operating increasingly closer to the Helmholtz resonance frequency as the cavity height is increased. To support this claim, CFD simulation using a static compressible model developed by Tang and Zhong [9] is performed to find the variation of the normalized vortex circulation with H/D_o, over the range of H tested in the present investigation. From Fig. 10, it can be seen that the normalized vortex circulation increases with cavity height, confirming the findings made from PIV. Although the magnitude of increase in circulation is not as large as that seen in Fig. 8, the compressible model does accurately depict the trend for both diaphragm displacements. This may also explain why opposite trends were obtained by the incompressible model [3], which cannot detect the effect of Helmholtz reasonance. In the case of Rizetta *et al* [4], where numerical simulations were used to solve the unsteady compressible Navier-Stokes equations for the cavity and external jet flow field, increasing vortex strength with decreasing cavity height was reported. However, it is likely that the actuator may have been operating away from the effects of resonance in the non-Helmholtz regime [9].

As such for increasing H/D_o in the present study, the effect of Helmholtz resonance becomes greater than the flow behaviour in the actuator, which could ultimately be responsible for the increase in vortex circulation obtained from experiment the static compressible model. Further discussions on how SJA performance can be maximized by Helmholtz resonance can be found in [9].

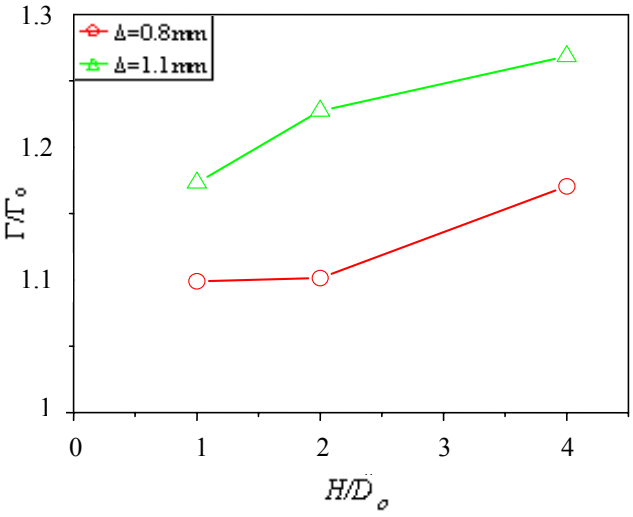

Fig 10. Correlation of normalized vortex circulation and H/D_o for h/D_o=1 obtained from compressible model [9]

5 Conclusions

PIV measurements have been undertaken to study the effects of varying orifice depth h and cavity height H on the magnitude of vortex circulation of round synthetic jets in quiescent conditions. It is found that at the same stroke length, the normalized vortex circulation increases rapidly with a decreasing h when h/D_o is less than 1 and appears to be constant for h/D_o greater than 1. A peak in the vortex circulation is observed for h/D_o=0.5. CFD simulations of the flow behaviour in the orifice duct reveal that this optimal h/D_o for the current actuator design corresponds to a minimum in the virtual exit diameter, as a result of the Vena Contracta moving out of the orifice.

For the same stroke length, an increase in the normalized vortex circulation is observed with increasing H/D_o. Simulation of the actuator design using a static compressible model reveals that for increasing H/D_o the effect of Helmholtz resonance becomes an increasingly more dominant feature and thus results in an increase in the vortex circulation. To summarise

- For varying h/D_o, the effects of the flow behaviour in the orifice are greater than the Helmholtz effect.
- For varying H/D_o, the effects of Helmholtz resonance are greater than the flow behaviour in the actuator.

The study has shown that the presence of the Helmholtz resonance can affect this type of investigation, however an improved understanding of how this phenomenon affects the jet velocity and vortex circulation has been achieved. The findings from this investigation ultimately provide useful information for optimizing the design of SJAs.

Acknowledgments

The authors would like to thank the EPSRC and the technician staff at the Goldstein Laboratory for their support of this work.

References

[1] Tang H and Zhong S. Incompressible Flow Model of Synthetic Jet Actuators. *AIAA Journal*, Vol. 44, No. 4, pp 908-912, 2006.

[2] Jabbal M, Wu J and Zhong S. The Performance of Round Synthetic Jets in Quiescent Flow. *The Aeronautical Journal*, to be published June 2006.

[3] Tang H and Zhong S. The Effect of Actuator Geometry on the Performance of Synthetic Jets. *CEAS/KATnet Conference on Key Aerodynamic Technologies*, Bremen, Germany, 20-22 June 2005.

[4] Rizzetta D.P, Visbal M.R and Stanek, M.J. Numerical Investigation of Synthetic Jet Flowfields. *AIAA Journal*, Vol. 37, No. 8, pp 919-927, 1999.

[5] Lee C.Y and Goldstein, D.B. Two-Dimensional Synthetic Jet Simulation. *AIAA Journal*, Vol. 40, No. 3, pp 510-516, 2002.

[6] Crook A and Wood N.J. A Parametric Investigation of a Synthetic Jet in Quiescent Conditions. *9th International Symposium on Flow Visualization*, Paper 67, Edinburgh, UK, 2000.

[7] Smith B.L and Glezer A. The Formation and Evolution of Synthetic Jets. *Physics of Fluids*, Vol. 10, No. 9, pp 2281-2297, 1998.

[8] Glezer A. The Formation of Vortex Rings. *Physics of Fluids*, Vol. 31, No. 12, pp 3532-3542, 1988.

[9] Tang H and Zhong S. Modelling of the Characteristics of Synthetic Jet Actuators. *35th AIAA Fluid Dynamics Conference and Exhibit*. AIAA Paper 2005-4748, Toronto, Canada, June 2005.